

Relation between effective conductivity and susceptibility of two-component rhombic checkerboard

This article has been downloaded from IOPscience. Please scroll down to see the full text article.

2003 J. Phys. A: Math. Gen. 36 5349

(<http://iopscience.iop.org/0305-4470/36/19/311>)

View [the table of contents for this issue](#), or go to the [journal homepage](#) for more

Download details:

IP Address: 171.66.16.103

The article was downloaded on 02/06/2010 at 15:29

Please note that [terms and conditions apply](#).

Relation between effective conductivity and susceptibility of two-component rhombic checkerboard

Leonid G Fel¹ and Ilia V Kaganov²

¹ School of Physics and Astronomy of Exact Sciences, Tel Aviv University, Ramat Aviv 69978, Israel

² Department of Chemical Engineering, Technion-IIT, Haifa 32000, Israel

Received 11 December 2002, in final form 21 March 2003

Published 29 April 2003

Online at stacks.iop.org/JPhysA/36/5349

Abstract

The heterogeneity of composite leads to extra charge concentration at the boundaries of different phases which results in essentially nonzero effective electric susceptibility. The relation between tensors of effective electric susceptibility $\hat{\chi}_{\text{ef}}$ and effective conductivity $\hat{\sigma}_{\text{ef}}$ of the infinite two-dimensional two-component regular composite with rhombic cell structure has been established. The degrees of electric field singularity at corner points of cells are found by constructing the integral equation for the effective conductivity problem. The limits of weak and strong contrast of partial conductivities σ_1, σ_2 are considered. The results are valid for thin films and cylindrical samples.

PACS numbers: 73.25.+i, 73.40.-c, 73.40.Jn, 73.50.-h, 73.61.-r

1. Introduction

The evaluation of effective properties for two-dimensional (2D) two-component composites, which determine the behaviour of the medium at large scales, given rise by Keller [1] and Dykhne [2], remains a topic of high activity. Among different approaches (variational bounds [3, 4], asymptotic [5, 6], numerical [7], network analogue [8, 9]) used to consider this problem, the analytical approach, being a classical problem of mathematical physics, is surprisingly very difficult. Exact values of effective parameters are of great interest even though these values are established in idealized models. It seems that explicit formulae are available only as exceptions. Such formulae which solve the field equations were obtained for a two-component regular checkerboard with square [10], rectangular [11, 12] and triangular [13] unit cells using complex-variable analysis. Another technique (integral equations) was used in recent papers dealing with square [14] and triangular [15] regular checkerboards.

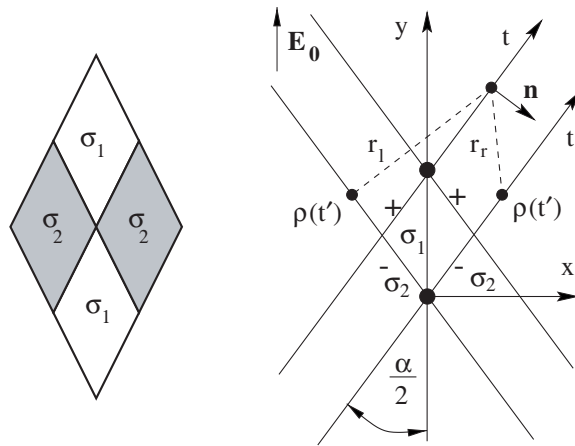


Figure 1. Regular rhombic two-component checkerboard under electric field E_0 : unit cell (left) and basic variables for integral equation (right). The distribution of the charges is drawn in accordance with chosen inequality $\sigma_1 \geq \sigma_2$.

Almost all these studies were directed towards effective conductivity σ_{ef} evaluation despite the important fact that the heterogeneity contributed to the conducting composite some dielectric properties. The homogeneous metal does not possess static dielectric properties (such as electric susceptibility) because only core electrons can contribute there, but their influence is obviously small. However, heterogeneity leads to extra charge concentration at the boundaries of different phases, which results in essentially nonzero effective electric susceptibility χ_{ef} . The implication follows that a relation between the conductivity $\hat{\sigma}_{\text{ef}}$ and susceptibility $\hat{\chi}_{\text{ef}}$ effective tensors must exist.

In the present paper we will consider the regular 2D two-component rhombic checkerboard and derive such a relation. This middle-symmetric structure belongs to the p'_cmm -plane group [16] and gives rise to an anisotropy of $\hat{\sigma}_{\text{ef}}$. In some sense this anisotropic model is more universal than the regular 2D two-component rectangular checkerboard ($c'mm$ -plane group). Really, the effective electric properties are mostly determined by the corner points of the cell, where the electric field is singular [5, 6]. The structure of a composite near these points in a rhombic checkerboard is governed by an *arbitrary* angular variable.

2. Integral equation

The regular checkerboard structure is composed of rhombic conducting cells with isotropic homogeneous conductivities σ_1 and σ_2 , hereafter $\sigma_1 \geq \sigma_2$. The backbone of such a structure can be represented as the set of images of the letter 'X' with infinitely long legs, which are shifted up and down to distance $2N \cos \frac{\alpha}{2}$, $N = 0, \pm 1, \pm 2, \dots$; α is the smallest angle between legs (see figure 1). The side of the cell is scaled by unit length. Such an arrangement of the checkerboard allows us to generate the kernel for the integral equation by single series summation rather than by double summation [14, 15].

We will consider the external unit field E_0 be applied in the vertical direction Y . It is one of the principal axes of the effective material tensors. Another axis X may be considered just by changing $\alpha \rightarrow \pi - \alpha$.

Let us proceed with solution of the Laplace equation for a scalar potential $\phi(r)$ at the infinite plane S

$$\phi(\mathbf{r}) = -E_0 y - 4\pi \int_S G(\mathbf{r}, \mathbf{r}_1) \rho(\mathbf{r}_1) d^2 r_1 \quad G(\mathbf{r}, \mathbf{r}_1) = \frac{1}{2\pi} \ln|\mathbf{r} - \mathbf{r}_1| \quad (1)$$

where $G(\mathbf{r}, \mathbf{r}_1)$ is the two-dimensional Green function and $\rho(\mathbf{r})$ is a charge distribution at the plane. The boundary conditions at the edge relate normal components of the field E_n and the current density j_n

$$E_n^{(1)} - E_n^{(2)} = 4\pi\rho(t) \quad j_n(t) = \sigma_1 E_n^{(1)} = \sigma_2 E_n^{(2)} \quad (2)$$

where a new variable t is introduced to measure the distance along the edge of a unit cell counted from the cell corner and $\rho(t)$ hereafter is the charge distribution at the edge. The boundary conditions (2) allow us to write the master equation

$$E_n^{(1)} + E_n^{(2)} = \frac{4\pi}{Z} \rho(r) \quad Z = \frac{\sigma_1 - \sigma_2}{\sigma_1 + \sigma_2} \quad 0 \leq Z \leq 1. \quad (3)$$

Finding the corresponding derivatives $E_n^{(i)}$ (see appendix A) we come to the integral equation

$$\frac{2\pi g(t)}{Z} \rho(t) = \sin \frac{\alpha}{2} - 4 \int_{-\infty}^{+\infty} \rho(t') K_1(t, t') dt' \quad (4)$$

where a new function $g(t)$ reflects a periodic interchange of the constituents (σ_1 and σ_2) with variation of argument t

$$g(t) = \text{sgn}[\text{mod}(t, 2) - 1] \quad g(-t) = -g(t) \quad g(t) = -1 \quad \text{for } 0 < t \leq 1 \quad (5)$$

the function $\text{mod}(t, 2)$ gives the remainder on division of t by 2 and $\text{sgn}[x]$ gives $-1, 0$ or 1 depending on whether x is negative, zero, or positive. The kernel $K_1(t, t')$ is given by the formula

$$K_1(t, t') = \sum_{k=-\infty}^{+\infty} \left[\frac{k}{(t-t')^2 \tan \frac{\alpha}{2} + (t-t'-2k)^2 \cot \frac{\alpha}{2}} + \frac{k+t'}{(t+t')^2 \tan \frac{\alpha}{2} + (t-t'-2k)^2 \cot \frac{\alpha}{2}} \right]. \quad (6)$$

It is worth representing the kernel for further summation as

$$K_1(t, t') = \frac{1}{4} \tan \frac{\alpha}{2} \sum_{k=-\infty}^{+\infty} \left[\frac{k}{(k-k_1)(k-k_1^*)} + \frac{k+t'}{(k-k_2)(k-k_2^*)} \right] \quad (7)$$

where the zeros k_1, k_1^* and k_2, k_2^* of both denominators in (6) read

$$k_1, k_1^* = \frac{t-t'}{2} \pm i \frac{|t-t'|}{2} \tan \frac{\alpha}{2} \quad k_2, k_2^* = \frac{t-t'}{2} \pm i \frac{|t+t'|}{2} \tan \frac{\alpha}{2}. \quad (8)$$

Making use of the identity

$$\frac{k+t'}{(k-k_i)(k-k_i^*)} = \text{Im} \left(\frac{k_i+t'}{k-k_i} \right) \frac{1}{\text{Im} k_i}$$

we can evaluate (7) in the sense of principal value and reduce essentially the kernel of integral equation (4)

$$K_1(t, t') = -\frac{\pi}{2} \text{Im} \left\{ \frac{k_1 \cot \pi k_1}{|t-t'|} + \frac{(k_2+t') \cot \pi k_2}{|t+t'|} \right\}. \quad (9)$$

The further simplification of the kernel $K_1(t, t')$ can be continued by usage of trigonometry. Introducing $\tilde{\rho}(t) = \rho(t)g(t)$ we obtain finally the integral equation

$$-\frac{2}{Z}\tilde{\rho}(t) = -\frac{1}{\pi}\sin\frac{\alpha}{2} + \int_{-\infty}^{+\infty}\tilde{\rho}(t')K_2(t, t')g(t')dt' \quad (10)$$

where

$$K_2(t, t') = \frac{\tan\frac{\alpha}{2}\sin\pi(t-t') - \sinh(\pi(t-t')\tan\frac{\alpha}{2})}{\cos\pi(t-t') - \cosh(\pi(t-t')\tan\frac{\alpha}{2})} + \frac{\tan\frac{\alpha}{2}\sin\pi(t-t') - \sinh(\pi(t+t')\tan\frac{\alpha}{2})}{\cos\pi(t-t') - \cosh(\pi(t+t')\tan\frac{\alpha}{2})}.$$

The function $\rho(t)$ being a solution of integral equation (10) makes it possible to find an exact expression of the effective conductivity tensor $\hat{\sigma}_{\text{ef}}$ (see section 4).

3. Asymptotic behaviour of $\rho(T)$ near the corners

We start this section with two algebraic properties of the function $\rho(t)$, which will be used in order to simplify further calculation. These are the parity and periodicity of the functions $\tilde{\rho}(t)$, $\rho(t)$, which are following from (10)

$$\tilde{\rho}(-t) = \tilde{\rho}(t) \quad \tilde{\rho}(t+2) = \tilde{\rho}(t) \longrightarrow \rho(-t) = -\rho(t) \quad \rho(t+2) = \rho(t). \quad (11)$$

They are in full agreement with the physics of the charge distribution $\rho(t)$ along the edges of the cells. A proof follows from an accurate evaluation of integral in (10). Indeed, the parity property follows due to (5) and identity $K_2(-t, -t') = -K_2(t, t')$,

$$\begin{aligned} \frac{2}{Z}\tilde{\rho}(-t) + \frac{1}{\pi}\sin\frac{\alpha}{2} &= -\int_{+\infty}^{-\infty}\tilde{\rho}(-t')K_2(-t, -t')g(-t')dt' \\ &= \int_{-\infty}^{+\infty}\tilde{\rho}(-t')K_2(t, t')g(t')dt'. \end{aligned} \quad (12)$$

The periodicity could be proved in a similar way.

A similar integral equation appeared in [14] for the two-component checkerboard with square unit cell. Its solution is presented by means of Weierstrass elliptic function $\rho_{sq}(t) \propto \wp^\kappa(t)$, where $\sin\pi\kappa = Z$, and is found by inspection of its behaviour near the branch points $t = 0$ and $t = 1$

$$E_n^{(i)}(t) \sim \rho_{sq}(t) \stackrel{t \rightarrow 0}{\sim} \frac{1}{t^{2\lambda_0}} \quad E_n^{(i)}(t) \sim \rho_{sq}(t) \stackrel{t \rightarrow 1}{\sim} (1-t)^{2\lambda_1} \quad \lambda_0 = \lambda_1 = \kappa. \quad (13)$$

The equality of the exponents $\lambda_0 = \lambda_1$ is here essential. Already the two-component checkerboard with triangle unit cell [15] breaks the validity of (13), that made an explicit unattainable³ solution, but only an efficient approximate method was proposed.

The rhombic structure, discussed in the present paper, also gives rise to distinct exponents. Asymptotic behaviour of $\rho(t)$ near the branch points $t = 0$ and $t = 1$ can be found from the equation (10) (see appendix A and figure 2)

$$E_n^{(i)}(t) \sim \rho(t) \stackrel{t \rightarrow 0}{\sim} \frac{1}{t^{2\mu_0}} \quad \sin\pi\mu_0 = Z\sin[\alpha + (\pi - 2\alpha)\mu_0] \quad (14)$$

$$E_n^{(i)}(t) \sim \rho(t) \stackrel{t \rightarrow 1}{\sim} (1-t)^{2\mu_1} \quad \sin\pi\mu_1 = Z\sin[\alpha + (2\alpha - \pi)\mu_1]. \quad (15)$$

³ The explicit solution of the effective conductivity problem for the two-component checkerboard composed of perfect triangles, was obtained in [13] where the conformal mapping of the triangle on the unit circle with a cut was used.

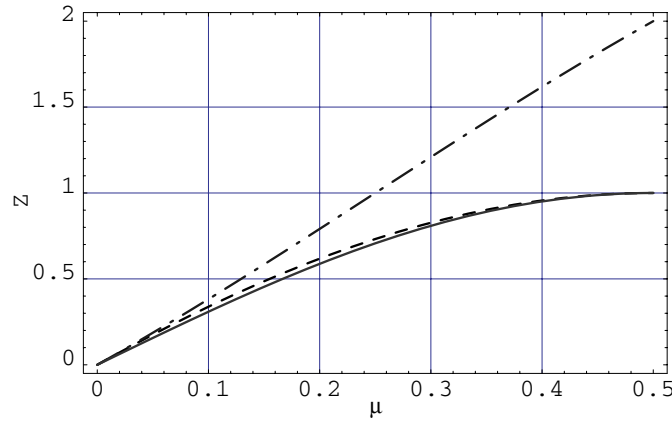


Figure 2. The branch point exponents $\mu_0(Z)$ (dashed line) and $\mu_1(Z)$ (dot-dashed line) for the rhombic unit cell with $\alpha = \pi/3$. The exponent $\kappa(Z)$ (full line) for the square unit cell is also presented.

Then

$$\begin{aligned} \mu_0(Z) = \mu_1(Z) = \kappa &= \frac{1}{\pi} \arcsin Z & \text{if } \alpha = \frac{\pi}{2} \\ \mu_0(Z) = -\mu_1(-Z) & & \text{if } \alpha \neq \frac{\pi}{2} \end{aligned} \quad (16)$$

and for a large contrast in conductivities $\sigma_2 \ll \sigma_1$, $Z \sim 1$: $2\mu_0 = 1$, $2\mu_1 = \alpha/(\pi - \alpha)$.

This shows that the generic rhombic cell ($\alpha \neq \frac{\pi}{2}$) does not lead to the solution of (10), which can be built out by simple rescaling of Weierstrass elliptic functions. An explicit solution of the integral equation remains to be performed.

It turns out that the integral equation (10), obtained in the present section, is sufficient to establish an exact relation between effective electric conductivity $\hat{\sigma}_{\text{ef}}$ and effective electric susceptibility $\hat{\chi}_{\text{ef}}$, which was not to our knowledge discussed earlier.

4. Effective susceptibility of a rhombic checkerboard

Let us consider the polarization of the rhombic checkerboard at scales large compared to the size of the cells. The effective electric susceptibility is the tensor which is defined by $\mathbf{P} = \hat{\chi}_{\text{ef}} \mathbf{E}$ where \mathbf{P} is polarization and \mathbf{E} is external electric field. In the reference frame (figure 1), when $\hat{\chi}_{\text{ef}}$ is diagonalized, its y -component is determined by the induced dipole moment d_y per unit square: $\chi_{\text{ef}}^y = d_y/S$, where

$$d_y = \sum_{\text{over all charges } q_j} y_j q_j = 2 \cos \frac{\alpha}{2} \sum_{k=-\infty}^{\infty} \int_{-\infty}^{\infty} (t+2k) \rho(t) dt \quad (17)$$

is the dipole moment of area $S = L_x L_y$ and L_x, L_y are the sizes of a sample. The summation covers all induced edge-charges q_j which are placed within the area S . The sample which is composed of $2N_x \times 2N_y$ unit cells has the area $S = 2N_x 2 \sin \frac{\alpha}{2} \times 2N_y 2 \cos \frac{\alpha}{2} = 8N_x N_y \sin \alpha$. Formula (17) can be reduced making use of parity and periodicity properties (11) of $\rho(t)$. Its accurate evaluation reads

$$d_y = 4N_y \cos \frac{\alpha}{2} \int_{-\infty}^{\infty} t \rho(t) dt = 4N_y \cos \frac{\alpha}{2} \sum_{n=-N_x}^{n=N_x} \int_{2n-1}^{2n+1} t \rho(t) dt = 8N_x N_y \cos \frac{\alpha}{2} \int_{-1}^1 t \rho(t) dt.$$

Taking into account the nonparity (5) of the function $g(t)$ we obtain finally

$$d_y = 16N_x N_y \cos \frac{\alpha}{2} \int_0^1 t \tilde{\rho}(t) dt \quad \text{and} \quad \chi_{\text{ef}}^y = \frac{1}{\sin \frac{\alpha}{2}} \int_0^1 t \tilde{\rho}(t) dt. \quad (18)$$

We also define the effective conductivity σ_{ef} as the ratio of the current $J = \int j_n(t) dt$ through the x -cross-section of the checkerboard per unit length to the applied field $E_0 = 1$

$$\sigma_{\text{ef}}^y = \frac{4\pi}{\sin \frac{\alpha}{2}} \frac{\sigma_1 \sigma_2}{\sigma_1 - \sigma_2} \int_0^1 \tilde{\rho}(t) dt \quad \sigma_{\text{ef}}^x(\alpha) = \sigma_{\text{ef}}^y(\pi - \alpha). \quad (19)$$

Due to Keller [1] the principal values of the tensor $\hat{\sigma}_{\text{ef}}$ satisfy the duality relations

$$\sigma_{\text{ef}}^x(\alpha) \cdot \sigma_{\text{ef}}^y(\alpha) = \sigma_1 \sigma_2. \quad (20)$$

Relating now two physical quantities (18), (19), we make use of auxiliary integral equation, obtained by integrating equation (10) (see appendix B)

$$\frac{\sigma_2}{\sigma_1 - \sigma_2} \int_0^1 \tilde{\rho}(t) dt = \frac{1}{4\pi} \sin \frac{\alpha}{2} - \int_0^1 t \tilde{\rho}(t) dt. \quad (21)$$

The last relation could be rewritten in new notation (18), (19),

$$4\pi \chi_{\text{ef}}^y = 1 - \frac{\sigma_{\text{ef}}^y}{\sigma_1} \quad \text{and similarly} \quad 4\pi \chi_{\text{ef}}^x = 1 - \frac{\sigma_{\text{ef}}^x}{\sigma_1}. \quad (22)$$

One can think that σ_1 , which appeared in (22), breaks the universality of the formulae. Actually, the denominator contains the maximal value of partial conductivities $\sigma_{\text{max}} = \max(\sigma_1, \sigma_2)$.

In fact, we have established the tensorial relation in any reference frame

$$4\pi \hat{\chi}_{\text{ef}} = \hat{I} - \frac{1}{\sigma_{\text{max}}} \hat{\sigma}_{\text{ef}} \quad (23)$$

where \hat{I} is an identity matrix. Formula (23) results in the particular square-checkerboard case: $4\pi \chi_{\text{ef}}^x = 4\pi \chi_{\text{ef}}^y = 1 - \sqrt{\sigma_2/\sigma_1}$.

Let us now consider two different cases of weak and large contrast in partial conductivities,

1. $(\sigma_1 - \sigma_2)/\sigma_1 \ll 1$, or $Z \ll 1$:

In first order on Z the integral equation (10) gives according to definition (19)

$$\rho(t) = -\frac{Z}{2\pi} \sin \frac{\alpha}{2} \rightarrow \sigma_{\text{ef}}^x = \sigma_{\text{ef}}^y = \sigma_1(1 - Z) \quad (24)$$

and therefore

$$4\pi \chi_{\text{ef}}^x = 4\pi \chi_{\text{ef}}^y = Z. \quad (25)$$

2. $\sigma_2 \ll \sigma_1$:

In this limit the corner points $t \rightarrow 0$ of the cell become important. Making use of the distribution (14) for the fields and charge $E_n^{(i)} \sim \tilde{\rho}(t) \sim t^{-2\mu_0}$ one can find approximately in leading terms

$$\mu_0 = \frac{1}{2} - \frac{1}{\sqrt{\alpha(\pi - \alpha)}} \sqrt{\frac{\sigma_2}{\sigma_1}} \rightarrow \sigma_{\text{ef}}^y = A \sqrt{\sigma_1 \sigma_2}. \quad (26)$$

Actually, the coefficient was found in [6]: $A = \sqrt{\alpha/(\pi - \alpha)} \cot(\alpha/2)$. Formula (26) implies as well

$$4\pi \chi_{\text{ef}}^x = 1 - A \sqrt{\frac{\sigma_2}{\sigma_1}} \quad 4\pi \chi_{\text{ef}}^y = 1 - \frac{1}{A} \sqrt{\frac{\sigma_2}{\sigma_1}}. \quad (27)$$

5. Conclusion

1. We have derived the integral equation for the effective conductivity problem for the regular 2D two-component rhombic checkerboard. Asymptotic behaviour of the electric field was investigated near the singular points $t = 0$ and $t = 1$.
2. The heterogeneity of composite leads to extra charge concentration at the boundaries of different phases that results essentially in nonzero effective electric susceptibility. The exact relation (23) between the two most important electrical properties, namely, effective conductivity $\hat{\sigma}_{\text{ef}}$ and effective susceptibility $\hat{\chi}_{\text{ef}}$, of the rhombic composite was established. An absence of specific angular parameter α in this formula makes it possible to conjecture its validity for any anisotropic two-component structure. It is shown that the tensor of electrical susceptibility has surprisingly simple structure in both cases of large and small contrast in partial conductivities σ_1, σ_2 .
3. The relation derived in the present paper is definitely valid for cylindrical samples. It is also valid for thin films due to the conducting nature of the constituents, which confine the electric field inside the conductor.
4. The electrical and magnetic properties of composites present current practical interest. These are mostly artificial mixtures (see e.g. [17]). Advances in technology permit the design of two-dimensional periodic composites even on a submicron scale [18]. Therefore, the relation (23) is of worth in the case when the direct measurement of the effective electric properties is difficult. On the other hand, if both effective electric susceptibility and conductivity are known, the relation allows one to get microscopic information, i.e. the conductivity of one of the constituents. It also may be used as a basic approximation for some kind of perturbation theory when the shape of cells is deviating from rhombic structure insignificantly. However, we conjecture that the relation is valid for any kind of two-component flat structure.

Acknowledgments

This research was supported in part by grants from the US–Israel Binational Science Foundation, the Israel Science Foundation, the Tel Aviv University Research Authority, Gileadi Fellowship program of the Ministry of Absorption of the State of Israel (LGF) and Israel Council for Higher Education (IVK).

Appendix A. Derivation of integral equation (4). Behaviour of its solution near the branch points

We define the variables

$$x = t \sin \frac{\alpha}{2} \quad y = t \cos \frac{\alpha}{2} \quad x' = \pm t' \sin \frac{\alpha}{2} \quad y' = t' \cos \frac{\alpha}{2} + 2k \cos \frac{\alpha}{2} \quad (\text{A.1})$$

and normal vector to the edge

$$\mathbf{n} = \left(\cos \frac{\alpha}{2}, -\sin \frac{\alpha}{2} \right). \quad (\text{A.2})$$

Here k is an ordinal number of the ‘X’ image. Keeping in mind the contributions from both left (l) and right (r) edges of the rhombic tile we will find the derivative

$$\partial\phi/\partial n = (\mathbf{n}\nabla)\phi$$

$$-\frac{\partial\phi}{\partial n} = E_0 \sin \frac{\alpha}{2} + \sum_{k=-\infty}^{\infty} \int_{-\infty}^{\infty} dt' \rho(t') \frac{1}{r_r^2(t, t')} \left(\frac{\partial r_r^2(t, t')}{\partial n} \right) \\ + \sum_{k=-\infty}^{\infty} \int_{-\infty}^{\infty} dt' \rho(t') \frac{1}{r_l^2(t, t')} \left(\frac{\partial r_l^2(t, t')}{\partial n} \right)$$

which leads after simple algebra to the equation

$$\frac{1}{2}(E_n^{(1)} + E_n^{(2)}) = -E_0 \sin \frac{\alpha}{2} + 4 \int_{-\infty}^{\infty} \rho(t') K_1(t, t') dt' \quad (\text{A.3})$$

where the kernel $K_1(t, t')$ reads

$$K_1(t, t') = \sum_{k=-\infty}^{\infty} \left[\frac{k}{(t-t')^2 \tan \frac{\alpha}{2} + (t-t'-2k)^2 \cot \frac{\alpha}{2}} \right. \\ \left. + \frac{t'+k}{(t+t')^2 \tan \frac{\alpha}{2} + (t-t'-2k)^2 \cot \frac{\alpha}{2}} \right]. \quad (\text{A.4})$$

Taking now $E_0 = 1$ we arrive at (4).

Below we consider the asymptotic behaviour of $\rho(t)$ near the branch points $t = 0$ and $t = 1$.

- $t \rightarrow 0$

Let us assume the power behaviour $\rho(t) \propto |t|^{-2\mu_0} \text{sgn}(t)$ and look for the exponent μ_0 . The main singularity comes from the integral in (10) in the vicinity $t' \rightarrow 0$. The kernel K_2 behaves as

$$K_2(t, t') \xrightarrow{t, t' \rightarrow 0} \frac{4}{\pi} \frac{t' \tan \frac{\alpha}{2}}{(t-t')^2 + (t+t')^2 \tan^2 \frac{\alpha}{2}} \quad (\text{A.5})$$

that gives the asymptotic behaviour

$$\frac{\rho(t)}{Z} = \frac{1}{\pi} \sin \alpha \int_{-\infty}^{+\infty} \frac{dt' t' \rho(t')}{t^2 + (t')^2 - 2t t' \cos \alpha}.$$

Defining a new variable $z = t'/t$ we obtain

$$\frac{\pi}{Z \sin \alpha} = \int_0^{+\infty} \frac{dz z^{1-2\mu_0}}{1+z^2-2z \cos \alpha} + \int_0^{+\infty} \frac{dz z^{1-2\mu_0}}{1+z^2+2z \cos \alpha}. \quad (\text{A.6})$$

The evaluation of the last expression is based on the primitive fraction expansion with further usage of standard integrals and gives finally (14).

- $t \rightarrow 1$

Let us assume the power behaviour $\rho(t) \propto |1-t|^{2\mu_1} \text{sgn}(1-t)$ and look for the exponent μ_1 . It is convenient to define new variables $\tau = 1-t$, $\tau' = 1+t'$ and consider the vicinity of the branch point $\tau \rightarrow 0$, so $\rho(t) \propto |\tau|^{2\mu_1} \text{sgn}(\tau)$. In order to deal with a singular part of the integral equation (10) let us differentiate the last over t

$$\frac{2}{Z} \frac{d\rho(t)}{dt} = \int_{-\infty}^{+\infty} \rho(t') \frac{dK_2(t, t')}{dt} dt' \quad \text{where} \quad \frac{d\rho(t)}{dt} \propto -2\mu_1(1-t)^{2\mu_1-1}. \quad (\text{A.7})$$

The main singularity comes from the integral in (A.7) in the vicinity $t' \rightarrow 1$, or $\tau' \rightarrow 0$, where the kernel behaves as

$$\frac{dK_2(t, t')}{dt} \xrightarrow{\tau, \tau' \rightarrow 0} -\frac{4 \sin \alpha}{\pi} \frac{\tau'(\tau + \tau' \cos \alpha)}{(\tau^2 + (\tau')^2 + 2\tau \tau' \cos \alpha)^2}. \quad (\text{A.8})$$

Defining a new variable $v = \tau'/\tau$ we obtain

$$\frac{\pi\mu_1}{Z \sin \alpha} = \int_0^{+\infty} \frac{dv v^{2\mu_1+1}(1+v \cos \alpha)}{(1+v^2+2v \cos \alpha)^2} + \int_0^{+\infty} \frac{dv v^{2\mu_1+1}(1-v \cos \alpha)}{(1+v^2-2v \cos \alpha)^2}. \quad (\text{A.9})$$

Evaluating the last integrals we arrive at (15).

Appendix B. Derivation of integral equation (21)

Recalling that the equation (10) is written in the sense of the principal integral value therein, we average this equation over the large interval $[-M, M]$, taking afterwards its limit $M \rightarrow \infty$

$$\frac{1}{2M} \int_{-M}^M \left[-\frac{2}{Z} \tilde{\rho}(t) + \frac{1}{\pi} \sin \frac{\alpha}{2} \right] dt = \frac{1}{2M} \int_{-M}^M dt \int_{-M}^M \tilde{\rho}(t') K_2(t, t') g(t') dt' \quad (\text{B.1})$$

where due to (11) the left-hand side reads

$$-\frac{2}{Z} \int_0^1 \tilde{\rho}(t) dt + \frac{1}{\pi} \sin \frac{\alpha}{2} \quad (\text{B.2})$$

while the right-hand side could be simplified. Indeed, let us represent the kernel $K_2(t, t')$ as follows:

$$\begin{aligned} K_2(t, t') &= \frac{(\tan \frac{\alpha}{2} + \cot \frac{\alpha}{2}) \sin \pi(t-t')}{\cos \pi(t-t') - \cosh[\pi(t+t') \tan \frac{\alpha}{2}]} + \frac{(\tan \frac{\alpha}{2} + \cot \frac{\alpha}{2}) \sin \pi(t-t')}{\cos \pi(t-t') - \cosh[\pi(t-t') \tan \frac{\alpha}{2}]} \\ &+ \frac{1}{\pi} \cot \frac{\alpha}{2} \frac{d}{dt} \ln \left\{ \cos \pi(t-t') - \cosh \left[\pi(t-t') \tan \frac{\alpha}{2} \right] \right\} \\ &+ \frac{1}{\pi} \cot \frac{\alpha}{2} \frac{d}{dt} \ln \left\{ \cos \pi(t-t') - \cosh \left[\pi(t+t') \tan \frac{\alpha}{2} \right] \right\}. \end{aligned} \quad (\text{B.3})$$

The last three terms do not contribute to integration of the kernel over t , while the first term implies

$$-\frac{2}{Z} \int_0^1 \tilde{\rho}(t) dt + \frac{1}{\pi} \sin \frac{\alpha}{2} = \frac{1}{2M} \int_{-M}^M \int_{-M}^M \tilde{\rho}(t') K_3(t, t') g(t') dt' dt \quad (\text{B.4})$$

where

$$\begin{aligned} K_3(t, t') &= \frac{2}{\sin \alpha} \frac{\sin \pi t}{\cos \pi t - \cosh(\pi(2t'+t) \tan \frac{\alpha}{2})} \\ &= -\frac{2}{\sin \alpha} \operatorname{Re} \left\{ \cot \frac{\pi}{2} \left[t + i(2t'+t) \tan \frac{\alpha}{2} \right] \right\}. \end{aligned} \quad (\text{B.5})$$

Continuing the integration of the kernel $K_3(t, t')$ we note that the function

$$F(t') = \lim_{M \rightarrow \infty} \int_{-M}^{+M} K_3(t, t') dt \quad (\text{B.6})$$

is a 1-periodic function: $F(t'+1) = F(t')$, which follows from the structure of the kernel $K_3(t, t')$. Evaluating the integral in (B.6) we arrive at the following:

$$F(t') = 2(1-2t') \quad \text{for } 0 \leq t' \leq 1. \quad (\text{B.7})$$

The final integral equation

$$2 \left(1 - \frac{1}{Z} \right) \int_0^1 \tilde{\rho}(t) dt + \frac{1}{\pi} \sin \frac{\alpha}{2} = 4 \int_0^1 t \tilde{\rho}(t) dt \quad (\text{B.8})$$

leads already to (21).

References

- [1] Keller J B 1964 *J. Math. Phys.* **5** 548
- [2] Dykhne A M 1970 *Sov. Phys.–JETP* **32** 63
- [3] Bergman D J 1978 *Phys. Rep. C* **43** 377
- [4] Milton G W 1981 *J. Appl. Phys.* **52** 5294
- [5] Keller J B 1987 *J. Math. Phys.* **28** 2516
- [6] Kozlov S M 1989 *Russ. Math. Survey* **44** 79
- [7] Helsing J 1991 *Phys. Rev. B* **44** 11677
Helsing J 1998 *J. Stat. Phys.* **90** 1461
- [8] Luck J M 1991 *Phys. Rev. B* **43** 3933
- [9] Fel L G and Khanin K M 2002 *J. Stat. Phys.* **108** 1015
- [10] Berdichevskii V L 1985 *Vestnik MGU, Math.* **40** 15
- [11] Obnosov Y V 1996 *Proc. R. Soc. A* **452** 2423
- [12] Milton G W 2001 *J. Math. Phys.* **42** 4873
- [13] Obnosov Y V 1999 *SIAM J. Appl. Math.* **59** 1267
- [14] Ovchinnikov Y N and Dyugaev A M 2000 *Sov. Phys.–JETP* **90** 881
- [15] Ovchinnikov Y N and Luk'yanchuk I A 2002 *Sov. Phys.–JETP* **94** 203
- [16] Belov N V 1956 *Kristallografia* **1** 621
- [17] Cohen R W, Cody G D, Coutts M D and Abeles B 1973 *Phys. Rev. B* **8** 3689
- [18] Yablonoitch E 1993 *J. Phys.: Condens. Matter* **5** 2443